A cation counterflux supports lysosomal acidification

Benjamin E. Steinberg,[1,2] Kassidy K. Huynh,[1,3] Alexandre Brodovitch,[1] Sabrina Jabs,[4] Tobias Stauber,[4] Thomas J. Jentsch,[4] and Sergio Grinstein[1,2,3]

[1]Program in Cell Biology, Hospital for Sick Children, Toronto, Canada M5G 1X8
[2]Institute of Medical Science and [3]Department of Biochemistry, University of Toronto, Ontario, Canada M5S 1A8
[4]Leibniz-Institut für Molekulare Pharmakologie (FMP) and Max-Delbrück-Centrum für Molekulare Medizin (MDC), D-13125 Berlin, Germany

The profound luminal acidification essential for the degradative function of lysosomes requires a counter-ion flux to dissipate an opposing voltage that would prohibit proton accumulation. It has generally been assumed that a parallel anion influx is the main or only counter-ion transport that enables acidification. Indeed, defective anion conductance has been suggested as the mechanism underlying attenuated lysosome acidification in cells deficient in CFTR or ClC-7. To assess the individual contribution of counter-ions to acidification, we devised means of reversibly and separately permeabilizing the plasma and lysosomal membranes to dialyze the cytosol and lysosome lumen in intact cells, while ratiometrically monitoring lysosomal pH. Replacement of cytosolic Cl⁻ with impermeant anions did not significantly alter proton pumping, while the presence of permeant cations in the lysosomal lumen supported acidification. Accordingly, the lysosomes were found to acidify to the same pH in both CFTR- and ClC-7–deficient cells. We conclude that cations, in addition to chloride, can support lysosomal acidification and defects in lysosomal anion conductance cannot explain the impaired microbicidal capacity of CF phagocytes.

Introduction

Lysosomes are the terminal compartment of the endocytic pathway. Their various acid hydrolases endow the organelle with the degradative capacity necessary to break down proteins, lipids, and polysaccharides. In certain cells, such as macrophages, lysosomes assume additional, specialized functions. Macrophages are important components of the innate immune response as they engage, internalize, and destroy invading microorganisms. In addition to homeostatic degradative functions, their lysosomes contribute antimicrobial capacities by fusing with the intracellular vacuole that ensnares the internalized pathogen. Most lysosomal hydrolases are optimally active in highly acidic solutions (Pillay et al., 2002), which mandates that the organellar lumen be maintained at pH values between 4 and 5. In macrophages, proton transport into phago-lysosomes also favors bacterial clearance by supporting NADPH oxidase activity, promoting the generation of toxic oxygen radicals and enhancing the activity of cationic microbicidal peptides. By regulating protease activity, the pH further controls antigen presentation and subsequent adaptive immune responses.

The pronounced acidification of the lysosomal interior is generated by the vacuolar-type ATPase (V-ATPase), a multimeric enzyme complex that utilizes the energy of ATP hydrolysis to translocate protons across membranes (Forgac, 2007). While the catalytic cycle of the V-ATPase drives proton accumulation, other factors contribute to the establishment of lysosomal acidification. The vectorial movement of protons across the membrane generates a transmembrane electrical potential difference (positive inside) that, if left uncompensated, curtails the activity of the V-ATPase and limits the magnitude of the pH gradient. To circumvent this self-limiting behavior, counter-ion conductive pathways must operate alongside the V-ATPase to dissipate the mounting voltage. Either the influx of cytosolic anions into the

The Rockefeller University Press $30.00
J. Cell Biol. Vol. 189 No. 7 1171–1186
www.jcb.org/cgi/doi/10.1083/jcb.200911083

JCB **1171**

organelle or the efflux of luminal cations can in principle serve as an electrical shunt to facilitate acidification.

Despite their importance to lysosomal acidification, the identity of the neutralizing counter-ions and their conductive channels in lysosomes remains elusive. Studies using pharmacological approaches alongside organellar pH measurements have largely focused on endosomes, and have implicated chloride as the principal counter-ion that dissipates the endosomal membrane potential generated by the V-ATPase. The intracellular CLC chloride channel family members ClC-3, ClC-4, and ClC-5 have been proposed as the primary endosomal chloride conductance providers (Günther et al., 1998, 2003; Piwon et al., 2000; Li et al., 2002; Mohammad-Panah et al., 2003; Hara-Chikuma et al., 2005a,b). ClC-7 is expressed in late endosomes and lysosomes (Kornak et al., 2001), but there is disagreement in the literature regarding its contribution to acidification (Kornak et al., 2001; Kasper et al., 2005; Lange et al., 2006; Graves et al., 2008). More recently, the cystic fibrosis (CF) transmembrane conductance regulator chloride channel (CFTR) was proposed as the specific counter-ion conductance necessary for lysosomal acidification in alveolar macrophages (Di et al., 2006). The lysosomes of CFTR-deficient macrophages were found to remain near neutrality, decreasing the capacity of these cells to clear a bacterial challenge (Di et al., 2006). The lung disease seen in CF was accordingly suggested to result in part from impaired lysosomal function. This mechanistic interpretation of CF pathobiology, however, has since been challenged (Haggie and Verkman, 2007; Lamothe and Valvano, 2008; Barriere et al., 2009).

Because of their central role in lysosome biology and potential involvement in the pathogenesis of CF, we analyzed the counter-ion pathways that support lysosomal acidification in macrophages using novel approaches to manipulate the ionic composition of the cytosol and of the lysosomal lumen in macrophages.

Results

The role of CFTR in lysosomal acidification

To investigate the counter-ions that support acidification, the lysosomes of murine macrophages were loaded with pH-sensitive dextrans and subjected to ratiometric imaging (Fig. 1, A and B). In the RAW264.7 and J774 macrophage lines, the steady-state lysosomal pH was 4.71 ± 0.04 and 4.52 ± 0.06, respectively (all values listed as mean ± SE; Fig. 1 C). As expected, lysosomal acidification was dissipated by concanamycin A (CcA), an inhibitor of the V-ATPase (pH ≥ 6.5, the upper limit of pH sensitivity of our sensor; Fig. 1, B and C). To evaluate its role in maintaining baseline pH, CFTR was pharmacologically inhibited by treating the cells for 1 h with the specific inhibitor CFTR$_{INH}$-172, which has been validated in multiple systems (Ma et al., 2002; Thiagarajah et al., 2004; Perez et al., 2007). No perturbation in steady-state lysosomal pH was observed in either cell line after treatment with the inhibitor (pH = 4.77 ± 0.06 and 4.51 ± 0.05 for RAW264.7 and J774 cells, respectively, at 5 µM CFTR$_{INH}$-172 and 4.82 ± 0.08 and 4.75 ± 0.11 at 10 µM; Fig. 1 C). Of note, the concentrations of CFTR$_{INH}$-172 used are

much greater than those required for full inhibition of CFTR (IC$_{50}$ ≈ 300 nM; Ma et al., 2002).

In the study by Di et al. (2006), CFTR was implicated in modulating lysosomal pH specifically in alveolar, but not other types of macrophages. To confirm this result, primary murine alveolar macrophages harvested by bronchoalveolar lavage were used to measure lysosomal pH. The steady-state pH (4.64 ± 0.02) was not significantly altered by incubation with 10 µM CFTR$_{INH}$-172 (4.75 ± 0.03; Fig. 1 D). That CFTR does not contribute importantly to lysosomal acidification was corroborated comparing alveolar macrophages from wild-type and CFTR-deficient mice. The lysosomal pH was virtually identical in wild-type and $cftr^{-/-}$ macrophages (4.64 ± 0.02 and 4.58 ± 0.06, respectively), and CcA fully dissipated acidification in both cases (Fig. 1 D). These observations rule out the possibility that residual CFTR activity, due to incomplete inhibition by CFTR$_{INH}$-172, provided the counter-ion conductance for lysosomal acidification.

Pharmacological inhibition of the V-ATPase with CcA unmasks a proton leak that gradually dissipates lysosomal acidification. Because net proton leakage requires translocation of a counter-ion, the rate of pH change caused by CcA can also be used to assess CFTR-mediated conductance in lysosomes. As shown in Fig. 1 E, the initial rates of lysosomal alkalinization in alveolar macrophages harvested from wild-type and $cftr^{-/-}$ mice were not significantly different (0.20 ± 0.01 min^{-1} and 0.16 ± 0.02 min^{-1}, respectively; P = 0.28), confirming that CFTR is not the predominant conductive pathway of the lysosomal membrane.

Role of ClC-7 in lysosomal acidification

Another Cl$^-$ conductance, the rheogenic 2Cl$^-$/H$^+$ antiporter ClC-7, has also been discussed in lysosomal acidification (Kornak et al., 2001; Graves et al., 2008). As shown in Fig. 2, A and B, ClC-7 is expressed in both RAW264.7 cells and in primary alveolar macrophages, where it colocalizes with the lysosomal marker LAMP-1 (Fig. S1). To address the possible involvement of ClC-7 in lysosome acidification, pH was measured in alveolar macrophages isolated from either wild-type or ClC-7 knockout mice (Kornak et al., 2001). Immunofluorescence determinations (Fig. 2 B) verified the absence of ClC-7 in the macrophages from knockout animals. As illustrated in Fig. 2 C, lysosomal pH in the macrophages of transporter-deficient $Clcn7^{-/-}$ animals (4.73 ± 0.12) was not significantly different from that in littermate controls (4.72 ± 0.24), in agreement with earlier ratiometric measurements of lysosomal pH in neurons and fibroblasts (Kasper et al., 2005; Lange et al., 2006). Fig. 2 C also shows that treatment of $Clcn7^{-/-}$ macrophages with CFTR$_{INH}$-172 inhibitor was without effect on baseline lysosome pH (4.72 ± 0.15), suggesting that anion conductance via CFTR does not become especially important in the absence of ClC-7.

Role of cytosolic anions in lysosomal acidification

Although we failed to implicate CFTR or ClC-7 as the primary counter-ion conductance pathways, cytosolic anions, mainly Cl$^-$, remained as leading candidates to provide the counter-charge for
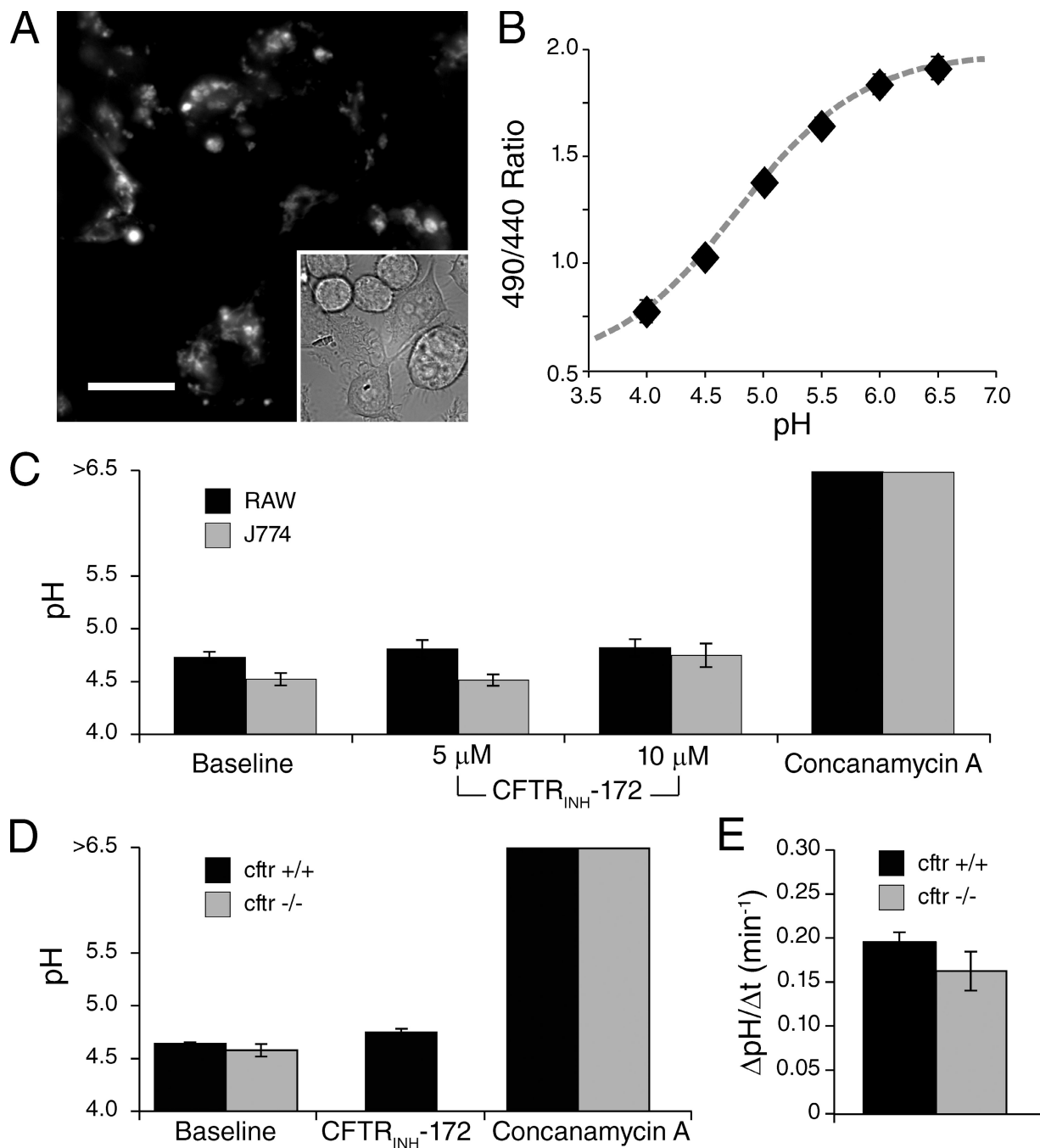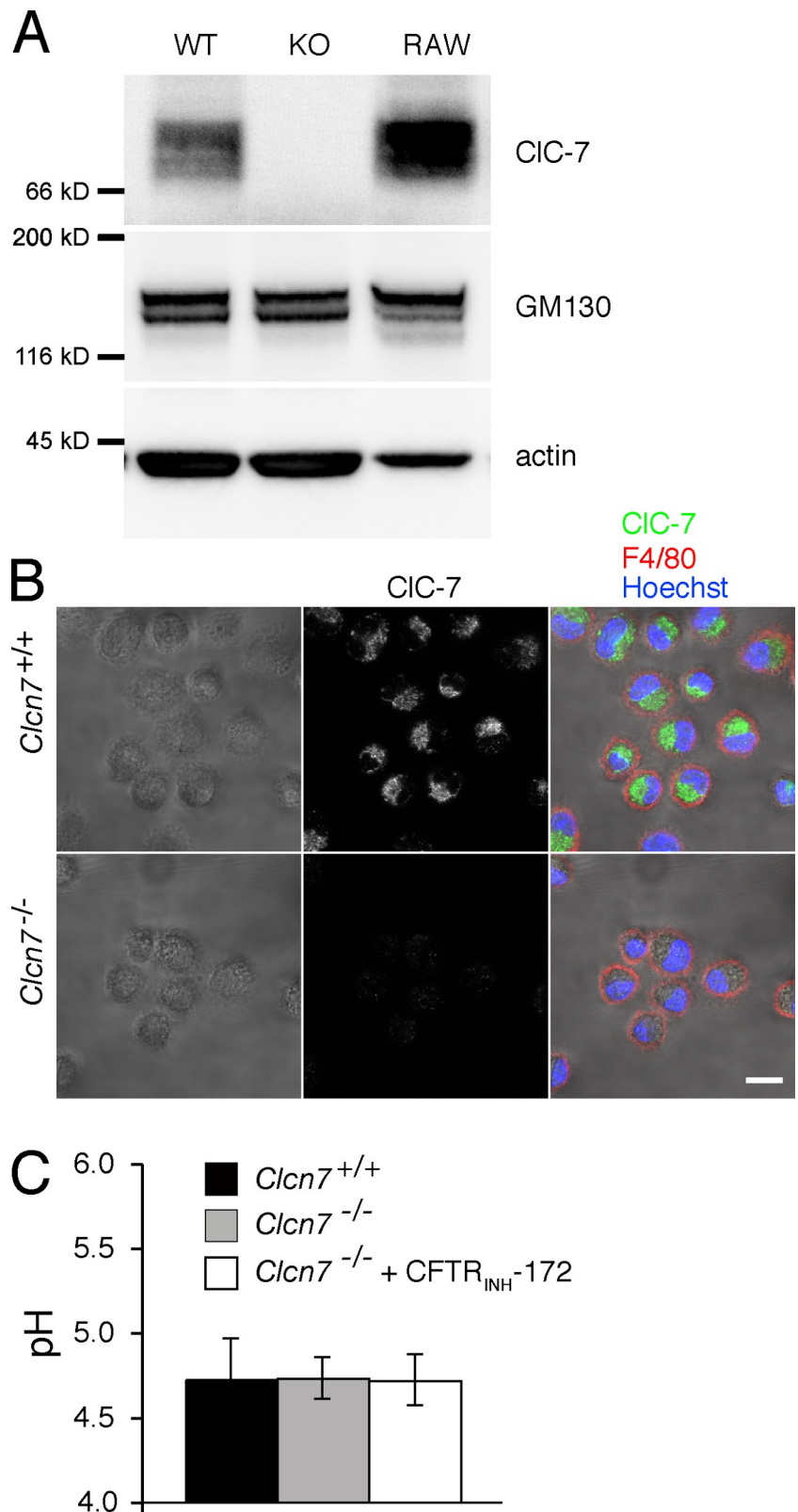
Figure 1. Steady-state lysosomal pH in macrophages. (A) The lysosomes of murine macrophages were loaded with pH-sensitive dextrans and their pH measured by ratiometric imaging. A representative field of RAW264.7 macrophages is shown in A (bar, 10 μm) with the corresponding differential interference contrast (DIC) image in the inset. At the end of each experiment, an in situ calibration was performed as described in Materials and methods to generate a curve relating the 490 nm/440 nm excitation ratio to pH (B). (C) The macrophage cell lines RAW264.7 (black bars) and J774 (gray bars) were either left untreated (5 experiments with a total of 669 lysosomes, and 5 experiments, 1103 lysosomes, respectively) or treated with 5 μM (3 experiments, 538 lysosomes; and 4 experiments, 810 lysosomes, respectively) or 10 μM (3 experiments, 304 lysosomes; and 4 experiments, 861 lysosomes, respectively) of the CFTR inhibitor CFTR$_{INH}$-172 for 1 h, and the lysosomal pH was recorded. In both cell lines, treatment with 500 nM CcA for 1 h dissipated the lysosomal pH to values greater than 6.5, the upper limit of sensitivity of the pH probe. (D) Lysosomal pH in alveolar macrophages harvested from wild-type or $cftr^{-/-}$ mice (5 experiments, 509 lysosomes; and 5 experiments, 395 lysosomes, respectively). Wild-type cells were also incubated for 1 h in the presence of 10 μM of CFTR$_{INH}$-172 (4 experiments, 450 lysosomes). (E) To determine whether CFTR functions as the counter-ion conductance for the proton leak in lysosomes, wild-type (3 experiments, 24 lysosomes) and $cftr^{-/-}$ (4 experiments, 34 lysosomes) alveolar macrophages were treated with 1 μM CcA and the rate of alkalinization was measured over the first 5 min.

proton uptake by lysosomes. To validate this notion we used a cytosolic ion-substitution protocol in combination with lysosomal pH measurements, as depicted schematically in Fig. 3 A. In brief, the plasma membrane of RAW macrophages was selectively permeabilized by stimulating resident P2X$_7$ receptors with the agonist 2′,(3′)-O-(4-benzoylbenzoyl)adenosine-5′-triphosphate (bzATP), a process validated earlier in this cell line by Pelegrin et al. (2008). Upon activation, P2X$_7$ receptors form large pores

Figure 2. **Expression of ClC-7 in alveolar macrophages: role in the establishment of lysosomal pH.** (A) The expression of ClC-7 in membranes isolated from fibroblasts of wild-type (WT) and ClC-7 knockout (KO) mice and in RAW264.7 macrophages was tested by immunoblotting, using the antibody described in Kornak et al. (2001). To verify comparable loading, the blots were also probed for the Golgi protein GM130 and for actin. (B) Alveolar macrophages obtained from wild-type ($Clcn7^{+/+}$) and ClC-7 knockout mice ($Clcn7^{-/-}$) were immunostained for ClC-7 (middle column; green in right column) and for the macrophage marker F4/80 (red in right column), and their nuclei stained with Hoechst 33342 (blue). Corresponding bright-field images are shown in the left column. Bar, 10 µm. (C) Lysosomal pH in alveolar macrophages harvested from wild-type (black bars) or $Clcn7^{-/-}$ mice without or with 10 µM CFTR$_{INH}$-172 (gray and white bars, respectively). Four experiments were performed per mouse type. For each experiment, at least 10 cells (each with ≥10 lysosomes) were measured.

through which molecules M_r ≤ 900 D are able to pass (Pelegrin and Surprenant, 2006). The well-defined, limited size of the P2X$_7$ mediated-pores and the fact that they close rapidly upon addition of divalent cations makes this an elegant and conservative means of manipulating the cytosolic ion content. By stimulating P2X$_7$ receptors while the cells are bathed in media where Cl$^-$ is replaced by organic anions such as gluconate or methanesulfonate (MeSO$_3^-$), the cytosolic Cl$^-$ can be dialyzed in exchange for the larger anions. Colorimetric Cl$^-$ determinations demonstrated that the total intracellular Cl$^-$ content decreased from 70.5 ± 4.2 mM
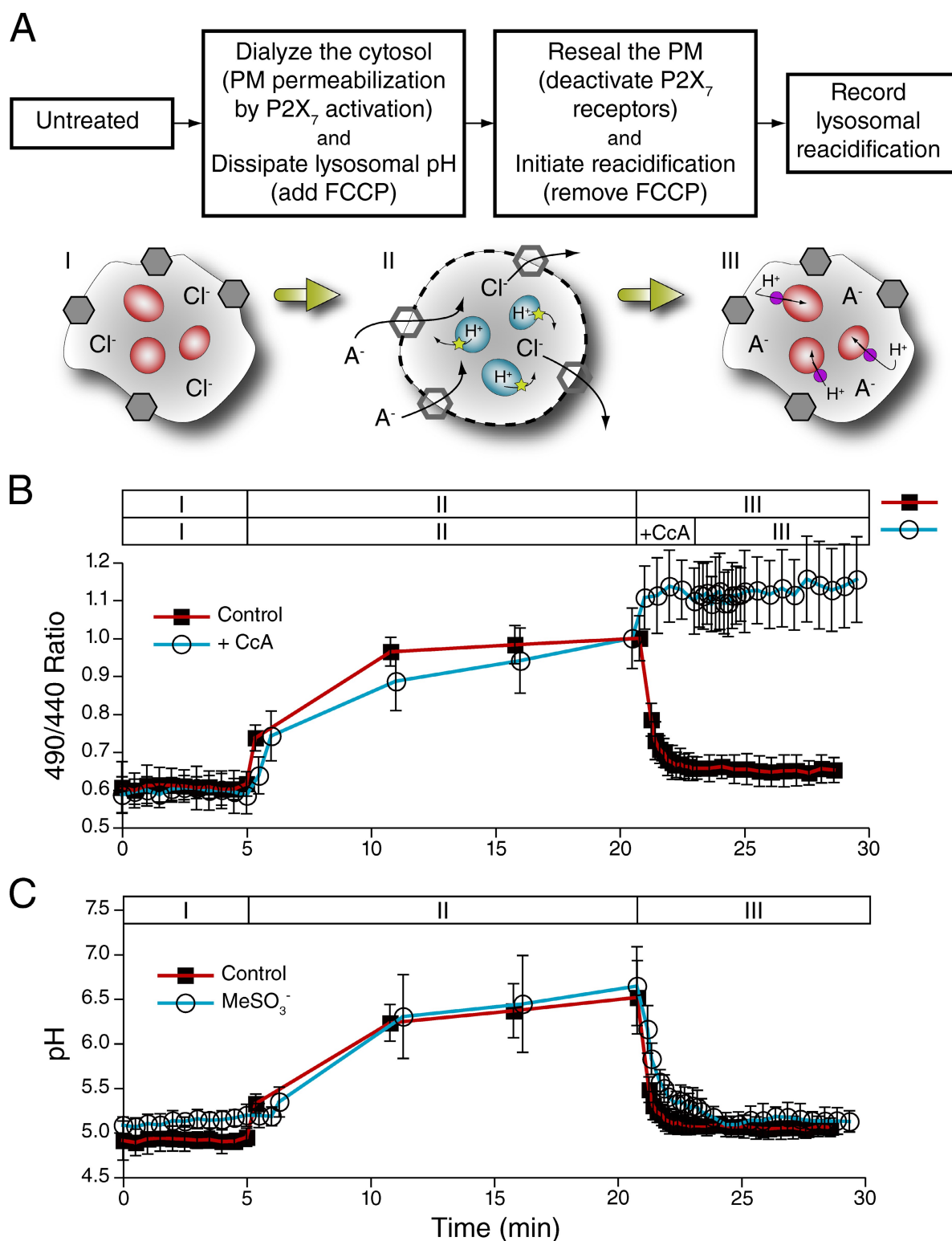
Figure 3. Role of cytosolic anions in lysosome re-acidification after protonophore-induced alkalinization. (A) Schematic representation of the experimental protocol used to dialyze cytosolic anions and transiently alkalinize lysosomes. After baseline pH measurements in RAW macrophages (step I), the cytosol was dialyzed by selectively permeabilizing the plasma membrane through the activation of P2X$_7$ receptors in the presence of anion substitution buffers (step II). Concurrently, the lysosomal pH was dissipated by treatment with the protonophore FCCP (step II). The plasma membrane was then resealed by removing the P2X$_7$ agonists and adding divalent cations, while lysosomal re-acidification was initiated by protonophore washout (step III). Lysosomal pH was monitored throughout the protocol. (B) Cells were subjected to the experimental protocol described in (A) while measuring pH. Representative recordings of the fluorescence ratio (proportional to pH) of untreated (filled squares) and CcA-treated cells (open circles) are illustrated (means ± SD of $n = 6$ and 9, respectively). The stages identified by the Roman numerals correspond to those in (A). Note that inhibition of the V-ATPase with CcA immediately before removal of FCCP fully abrogated lysosomal re-acidification. (C) Cytosolic anion substitution with MeSO$_3^-$ did not change the rate or extent of lysosome re-acidification. Representative traces of control (filled squares) and anion-substituted (open circles) cells are shown (means ± SD of $n = 6$). Summary statistics are presented in Table I.

Table I. **Rate and extent of lysosome re-acidification after cytosolic anion dialysis and protonophore-induced alkalinization**

	n	τ (min)	$pH_f - pH_o$	$pH_{alk} - pH_f$
Control	16	0.68 ± 0.07	-0.01 ± 0.03	0.91 ± 0.09
Gluconate$^-$	6	0.44 ± 0.02 (P > 0.05; NS)	-0.03 ± 0.03 (P > 0.05; NS)	0.72 ± 0.17 (P > 0.05; NS)
MeSO$_4^-$	6	0.69 ± 0.06 (P > 0.05; NS)	0.09 ± 0.05 (P > 0.05; NS)	1.31 ± 0.05 (P < 0.05)
CFTR$_{INH}$-172	5	1.34 ± 0.25 (P < 0.01)	-0.17 ± 0.10 (P > 0.05; NS)	0.71 ± 0.07 (P > 0.05; NS)

The differences between the initial lysosome pH (pH_o; step I of the protocol shown in Fig. 3 A), pH after protonophore-induced alkalinization (pH_{alk}; step II of the protocol in Fig. 3 A), and final pH after re-acidification (pH_f; step III of the protocol in Fig. 3 A) were calculated. To determine the half-life of the pH decay (τ) the data for lysosome re-acidification after protonophore washout were fit to a single exponential of the form $y = A * \exp(-K x) + B$ and τ calculated as $0.69/K$. All values are listed as mean ± SE. The p-values, given in parentheses, were determined by ANOVA using Dunnett's test for multiple comparison to the control (NS, not significant). n refers to the number of experiments performed for each condition. For each experiment, 6–13 regions of interest were measured.

to 8.5 ± 1.7 mM after 15 min of bzATP treatment in media devoid of Cl$^-$ (Fig. S2, A and B). The remaining Cl$^-$ reflects a pool of slowly exchangeable or nonexchangeable organellar Cl$^-$. This was concluded from determinations of Cl$^-$ released by bzATP into the medium, which is maximal in the first 5 min and negligible after 15 min

To optimize detection of V-ATPase–induced acidification, the lysosomes were transiently alkalinized using the protonophore carbonyl cyanide 4-(trifluoromethoxy)phenylhydrazone (FCCP) concurrently with the cytosolic dialysis step. Re-acidification was then initiated by removal of the protonophore, which was effected concomitantly with the closure of P2X$_7$-induced pores. When the dialysis medium contained 50 mM Cl$^-$ to mimic the normal Cl$^-$ content of the cytosol, lysosomes rapidly re-acidified to baseline values after plasma membrane resealing and protonophore washout (Fig. 3 B). Notably, the re-acidification was inhibited by addition of CcA immediately before protonophore washout (Fig. 3 B), verifying that the drop in pH is due to the activity of the V-ATPase. Consistent with our previous results, treatment with 10 µM CFTR$_{INH}$-172 did not alter the extent of re-acidification, though the rate was reduced by ∼50% (Table I). The mechanism underlying the reduction in rate is unclear; although it may reflect a contribution of CFTR to the counter-ion conductance, we regard this possibility as unlikely in view of the earlier results obtained using $cftr^{-/-}$ mice. CFTR$_{INH}$-172 may be blocking other counter-ion pathways or inducing a proton leak that partially offsets the rate of acidification. More importantly, replacement of cytosolic Cl$^-$ with either MeSO$_3^-$ (Fig. 3 C) or gluconate (unpublished data) had no discernible effect on either the rate or extent of re-acidification (Table I). It follows that Cl$^-$ and other small cytosolic anions are not absolutely necessary for lysosome acidification. As both MeSO$_3^-$ and gluconate are poorly permeable through CFTR (Linsdell et al., 1997), these data lend further evidence against CFTR as the counter-ion conductance.

Although our determinations indicate that during the ion-substitution studies minimal Cl$^-$ remained in the cytosol after dialysis, it is possible that a small amount of residual Cl$^-$ contributed to the rapid re-acidification kinetics. To address this possibility, we performed in vitro experiments measuring the pH of isolated lysosomes in a cell-free system. To this end, the lysosomes of RAW macrophages were first labeled with dextran conjugated to a fluorescent pH sensor, using a pulse-chase loading protocol.

Selective labeling of the lysosomes obviated the need for extensive purification of these organelles, which is time consuming and can result in swelling and alteration of permeability properties. The pH gradient across the lysosomal membrane was then dissipated by treatment with the protonophore FCCP, the cells were homogenized, and the endomembrane compartments isolated through centrifugation. During protonophore treatment and organelle isolation the cells and homogenate were maintained either in Cl$^-$-containing medium or in a medium where all Cl$^-$ was substituted by gluconate. The pH of the isolated lysosomes was monitored in the corresponding solution using a fluorescence spectrometer. After a baseline measurement, ATP and Mg were added to the endomembrane suspension to activate the V-ATPase and initiate acidification, while continually monitoring fluorescence. As shown in Fig. 4 A, when maintained in the presence of Cl$^-$ the isolated lysosomes retained the ability to re-acidify, as indicated by quenching of the fluorescence. Subsequent addition of the K$^+$/H$^+$ exchanger nigericin restored the original fluorescence, implying that the lysosomes remained intact and suggesting that ATP-Mg had indeed altered the luminal pH. Accordingly, when added in the presence of CcA, ATP-Mg failed to induce the acute acidification noted above (Fig. 4 B). Most notably, lysosomes that were isolated and maintained in medium devoid of Cl$^-$ were similarly capable of acidifying and this response was equally sensitive to CcA, implying mediation by the V-ATPase (Fig. 4 B). Together, these observations confirm our earlier conclusion that permeant anions are dispensable for lysosome acidification.

It is important to note that the lysosomal membrane does possess a considerable Cl$^-$ conductance that, while not absolutely required for acidification, can nevertheless support it. In agreement with earlier observations, the ability of Cl$^-$ to support proton translocation was revealed when comparing the re-acidification of isolated lysosomes suspended in a sucrose-based medium either devoid of all permeant ions or supplemented with Cl$^-$. To minimize their contribution, luminal cations were depleted by incubating the intact macrophages in a Na$^+$- and K$^+$-free, N-methyl-D-glucammonium (NMDG$^+$)–based medium for 1 h before isolating the lysosomes. Whether the lysosomes undergo shrinkage during the depletion protocol remains unclear; volume loss could be minimized by generation of proteolytic products or by slow uptake of NMDG$^+$ during the prolonged depletion period. When internal Na$^+$ and K$^+$ were depleted proton pumping by the V-ATPase could not be sustained when permeable anions
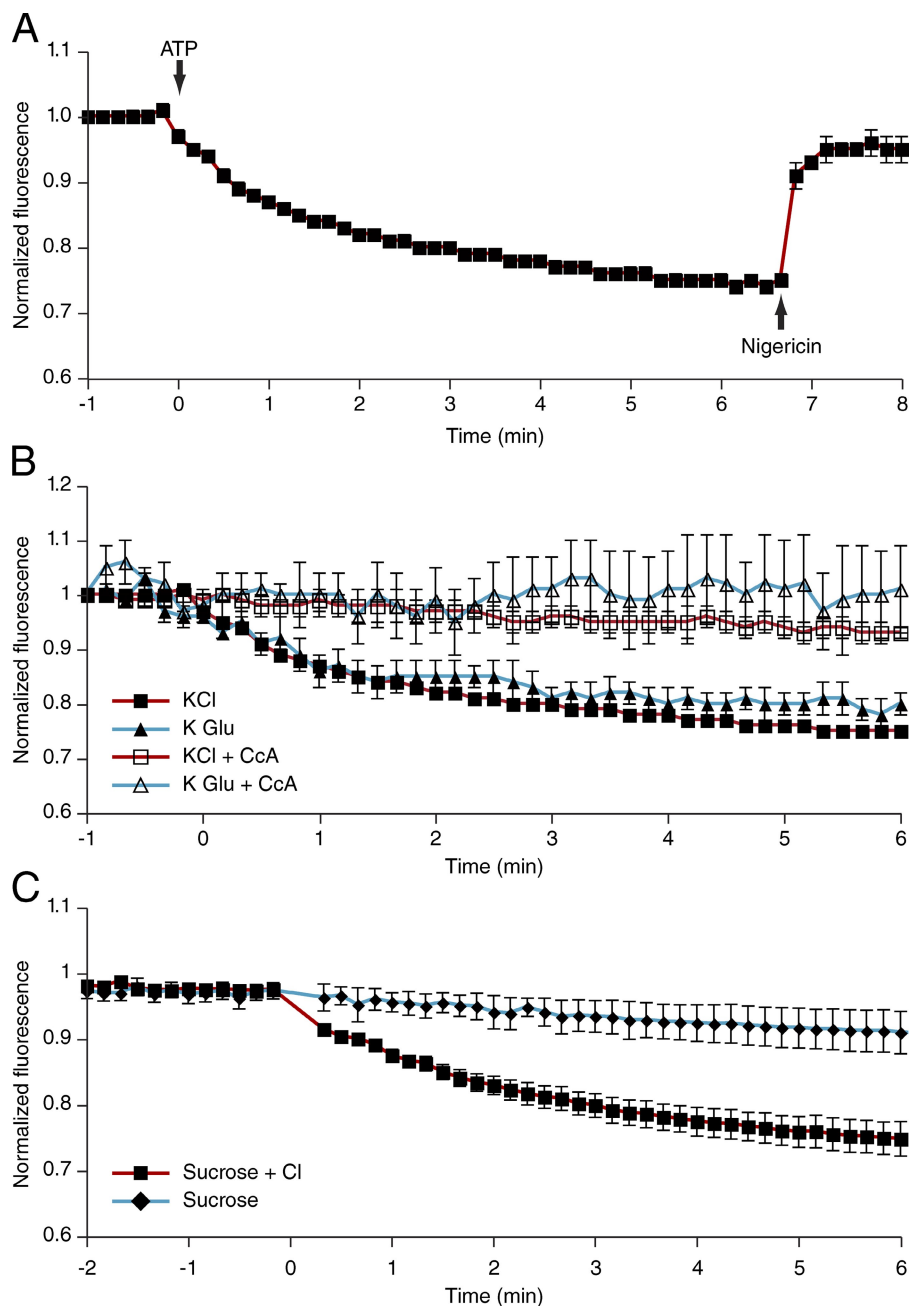
Figure 4. Role of anions in the acidification of isolated lysosomes. (A) The pH of isolated RAW macrophage lysosomes bathed in Cl⁻-containing medium was monitored by fluorescence spectrometry as described in the text. The pH gradient across the lysosomal membrane was intentionally dissipated during the course of isolation. Where indicated, lysosomal re-acidification was initiated by addition of ATP-Mg. Finally, nigericin was added to release the accumulated H⁺. (B) Isolated lysosomes were bathed in either Cl⁻-based (black squares) or gluconate-based (black triangles) medium and ATP-Mg was added as in A to initiate re-acidification. Where indicated, CcA was added concomitantly. Data are means ± SE of at least three separate experiments of each kind. Lysosomes had undergone significant acidification at 5 min after the addition of MgATP as compared with CcA controls (P = 0.007 and P = 0.0159 for the Cl⁻- and gluconate-based solutions, respectively). (C) Macrophages were incubated in medium devoid of small, monovalent cations (i.e., K⁺ and Na⁺) for 1 h. The lysosomes were then isolated in either a sucrose-based medium or a sucrose-based medium containing Cl⁻. In both cases, the media were devoid of K⁺ and Na⁺. Re-acidification was initiated as above by addition of ATP-Mg. Data are means ± SE of at least three separate experiments of each kind for panels B and C.
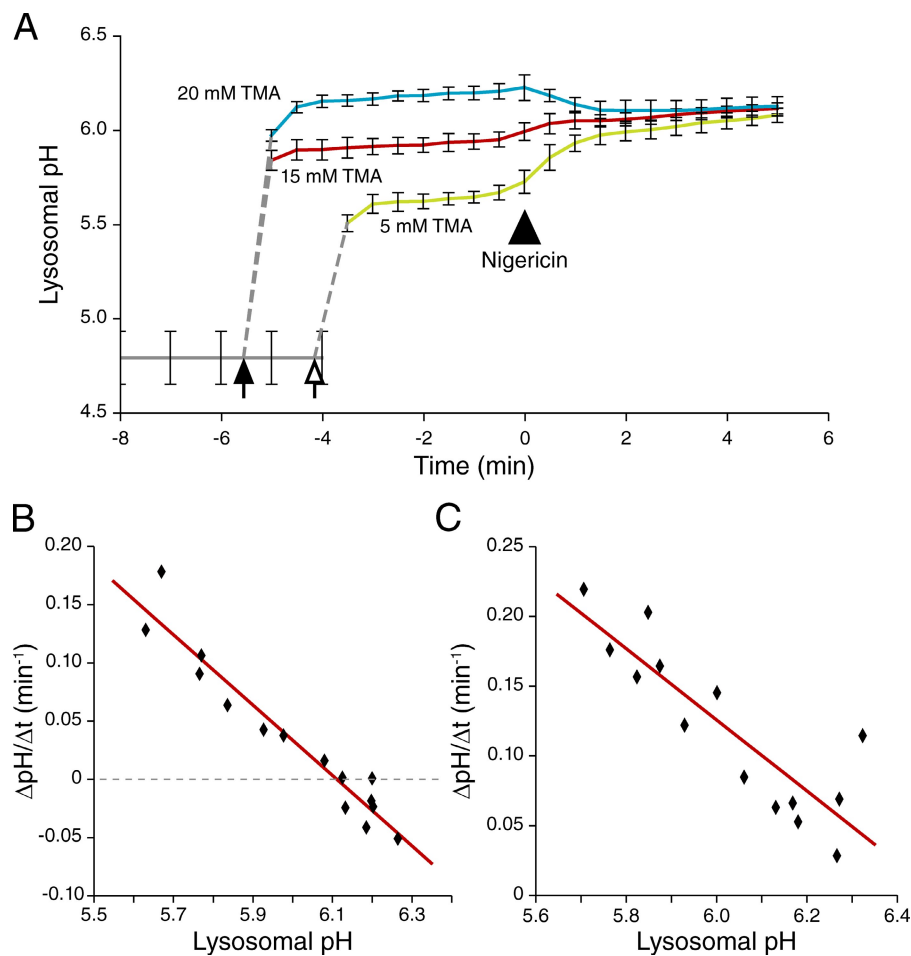
were omitted from the medium (Fig. 4 C), implying that any residual luminal cations were negligible contributors to the counter-ion flux. In the presence of Cl⁻, however, lysosomes were able to acidify upon the addition of MgATP (Fig. 4 C).

Lysosomal K⁺ and Na⁺ determinations by null-point titration

Because our evidence suggested that cytosolic anions are not absolutely required as counter-ions we considered whether luminal cations can also support lysosomal acidification. To date, the presence and in particular the concentration of free cations inside lysosomes has not been established, likely because the spectroscopic probes of cation activity are incompatible with the extreme acidity of the lysosomal lumen. Instead, we implemented a method that uses ionophores that exchange monovalent

cations for protons with defined stoichiometry to indirectly assess cation activity. Based on the theoretical considerations summarized in the Materials and methods, the steady-state free concentration of Na⁺ and K⁺ can be estimated by means of a "null-point" titration of lysosomal pH. This required manipulation of the cytosolic monovalent cation concentration, which was accomplished by reversible activation of plasmalemmal P2X₇ receptors, as described above, followed by graded alkalinization of the lysosomal lumen using the weak base trimethylamine (TMA). Three representative traces using different amounts of TMA for K⁺ determination with nigericin are shown in Fig. 5 A. From multiple such determinations we estimated the null-point, i.e., the lysosomal pH at which ΔpH/Δt = 0 (Fig. 5 B), which was in turn used to calculate K⁺ activity as detailed in Materials and methods. From 15 independent determinations at

Figure 5. **Null-point titration determinations of lysosomal K⁺ and Na⁺.** Estimates of lysosomal K⁺ and Na⁺ in live RAW macrophages were obtained using the null-point method, as described in Materials and methods. Lysosomes were loaded with a pH-sensitive dextran, and the cytosolic and extracellular compartments equilibrated using bzATP-activated P2X₇ receptors. The lysosomes were alkalinized with the specified amount of TMA (20 mM or 15 mM TMA added where indicated by the filled arrow, and 5 mM TMA where indicated by the open arrow). Changes in lysosome pH upon the addition of a cation/proton exchanging ionophore were measured next to find the null-point, i.e., the condition when addition of the ionophore elicits no change in pH. In the experiments shown in A, nigericin was added to all samples at 0 min (filled arrowhead). The traces are means ± SD of three representative experiments. For each null-point titration experiment, the rate of pH change (ΔpH/Δt) after addition of the ionophore was measured over 90 s and plotted as a function of the lysosome pH at the time of addition of the ionophore. The data obtained using nigericin and monensin, used to estimate K⁺ and Na⁺ as detailed in Methods, are shown in B and C along with the calculated least-squares linear regressions ($R^2 = 0.9272$ and $R^2 = 0.7509$ for panels B and C, respectively).

pH 6.5, each measuring between 6 and 8 lysosomes, we determined the free [K⁺] in the lumen of lysosomes to be 50.1 ± 2.0 mM. To confirm the reliability of this determination we conducted a second null-point titration at pH 7.3 (Fig. S2 D). Elevating the cytosolic pH is expected to change the value of the null-point, but should nevertheless yield an estimate of the lysosomal K⁺ content comparable to that calculated at pH 6.5. Using the data obtained at cytosolic pH 7.3 we calculated a null-point of pH 6.81 ± 0.04 corresponding to a luminal K⁺ content of 61.7 ± 6.2 mM, in reasonable agreement with the value estimated at pH 6.5.

Although nigericin is selective for K⁺/H⁺ exchange, monensin, the ionophore used in the Na⁺ null-point titration, is only moderately selective. It preferentially exchanges Na⁺ for H⁺ but is also capable of mediating K⁺/H⁺ exchange with reduced efficiency. To calculate intra-lysosomal Na⁺ activity the lysosomal [K⁺], which was determined independently, and the selectivity coefficient of the ionophore were also taken into account (see Materials and methods). From monensin null-point titrations shown in Fig. 5 C, and using the lysosomal [K⁺] determined above, we estimate intra-lysosomal free [Na⁺] to be 20.6 ± 2.1 mM. Considering the lysosomal buffering capacity (61.5 ± 2.3 mM/pH at pH 4.5–5; $n = 10$ experiments), it is clear that the aggregate content of monovalent cations is sufficient to support lysosomal acidification by over 1 pH unit and/or its maintenance in the steady state.

Role of luminal cations in lysosomal acidification

To investigate whether luminal cations are capable of generating and maintaining lysosomal acidification, we used an ion-substitution strategy. Unlike the approach used to study anions, however, these experiments required manipulation of the internal cation content of the lysosomes. This was accomplished by transient permeabilization of the lysosomal membrane using the dipeptide Gly-Phe-β-naphthylamide (GPN), a compound previously used to dissipate and study the regulation of lysosomal Ca²⁺ (Berg et al., 1994; Haller et al., 1996a,b; Srinivas et al., 2002; McGuinness et al., 2007). This membrane-permeant reagent diffuses into lysosomes where it is cleaved by cathepsin C, an exopeptidase found exclusively in these organelles (Jadot et al., 1984). The osmotically active products accumulate, drawing water into the lumen and leading to organelle swelling. When its ability to distend is exceeded, the lysosomal membrane undergoes a transient permeabilization. Under the conditions chosen for our experiments, the pore size generated by the permeabilization procedure is limited. Large molecules such as dextrans are retained by the lysosomes (Fig. 6 B), whereas smaller compounds like sulforhodamine (Mᵣ = 607), and by extension small inorganic cations, are released (Fig. 6 A). As a result the pH of the lysosomal lumen equilibrates with that of the surrounding cytosol, and the lysosomes fail to accumulate LysoTracker (Fig. 6 C). Remarkably, after short (10 min) exposure periods to GPN, the permeabilization process can be
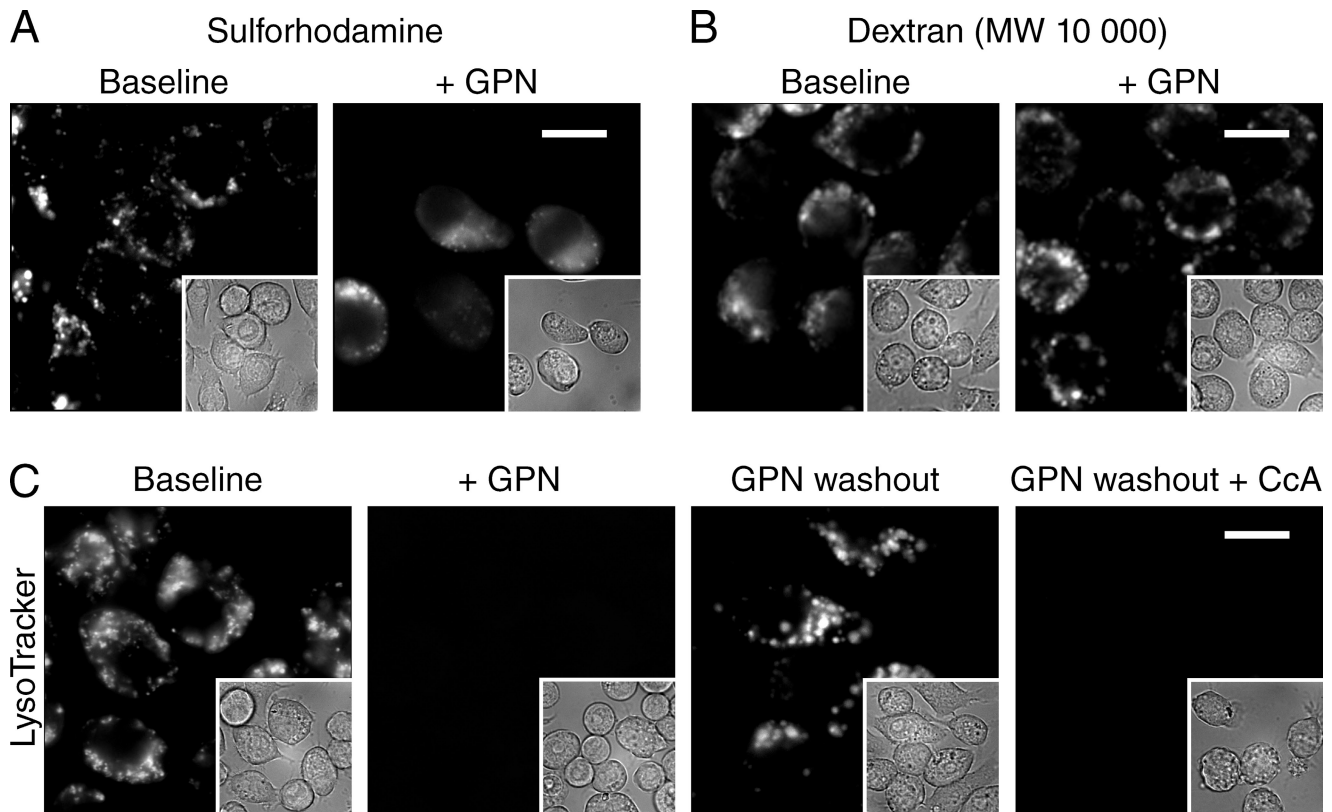
A Sulforhodamine — Baseline / + GPN

B Dextran (MW 10 000) — Baseline / + GPN

C LysoTracker — Baseline / + GPN / GPN washout / GPN washout + CcA

Figure 6.   **GPN-induced transient lysosome membrane permeabilization.** Lysosomes of RAW264.7 macrophages were loaded with either (A) sulforhodamine or (B) fluorescently labeled dextrans (MW 10,000), and imaged before and after 10 min of GPN treatment. Corresponding DIC images are shown in the insets. (C) The pH of the lysosomes was monitored qualitatively using LysoTracker, which accumulates in acidic intracellular compartments. The dye was added to the cells either before GPN treatment, after 10 min of GPN treatment, or after 10 min of recovery subsequent to 10 min of GPN treatment. Dye accumulation was abrogated when CcA was added to the cells immediately after GPN washout. Representative fields (Bar, 10 µm) are shown along with their corresponding DIC images (insets).

reversed by removal of the dipeptide. Within minutes of GPN washout the lysosomes recover the ability to accumulate the acidotropic dye and the recovery is precluded by CcA (Fig. 6 C), implying that it reflects renewed proton pumping by the V-ATPase.

This transient permeabilization protocol enabled us to manipulate the ionic content of the lysosomal lumen to assess the role of monovalent cations in acidification. A schematic of the lysosome dialysis and alkalinization protocol is shown in Fig. 7 A. The baseline lysosomal pH was initially monitored in cells loaded with indicator probes (step I). The plasma membrane was then selectively permeabilized by $P2X_7$ activation and the cytosol dialyzed while bathing the cells in either a cytosol-like (K^+-rich control) or cation-substituted medium (step II). To gain insight into the kinetics of cytosolic cation dialysis, K^+ was monitored using the fluorescent K^+ probe PBFI. When $P2X_7$ receptors were stimulated in a K^+-rich solution, no change in K^+ content was observed. In contrast, when the cells were bathed in an $NMDG^+$-rich solution during $P2X_7$ activation, intracellular K^+ was rapidly depleted within 10 min of dialysis (see Fig. S2 C). Accordingly, the cytosol dialysis (step II) was performed for 15 min. After cytosolic dialysis the plasma membrane was resealed by deactivating the $P2X_7$ receptors and the cells allowed 5 min to recover (step III). For the remainder of the experiment, the cells were bathed in the same medium used for cytosolic dialysis, except that the

$P2X_7$ agonist was removed and divalent cations were re-added. The lysosomes were next dialyzed (and inevitably alkalinized) by treatment with GPN (step IV). Finally, GPN was removed and the ability of lysosomes to re-acidify was monitored after 10 min (step V). The results of a representative control experiment, where a cytosol-like (K^+-rich) solution was used during the dialysis, are shown in Fig. 7 B (the Roman numerals refer to the corresponding steps in the protocol schematic of Fig. 7 A). Comparable experiments using either an $NMDG^+$-based dialysis solution or $NMDG^+$-based solution without the cytosolic dialysis step are illustrated in Fig. S3.

To evaluate the extent of re-acidification observed after lysosomal cation dialysis followed by removal of GPN, we constructed histograms of pooled lysosome pH determinations from multiple experiments (Fig. 7 C). When K^+ was resealed into the lysosomes, mimicking the conditions prevailing physiologically, the lysosomes acidified back to pH = 5.44 (median of 1,349 determinations), approaching the normal resting value. In stark contrast, lysosomes dialyzed with Na^+- and K^+-free solutions, containing either Tris or $NMDG^+$, were unable to re-acidify (median re-acidification pH > 6.5 and 6.26 for Tris and $NMDG^+$, respectively). The inability to acidify was not the result of untoward deleterious effects of the organic cations because when the ion-substitution protocol was performed in the absence of bzATP, and thus without actually dialyzing the cytosol and lysosome lumen,
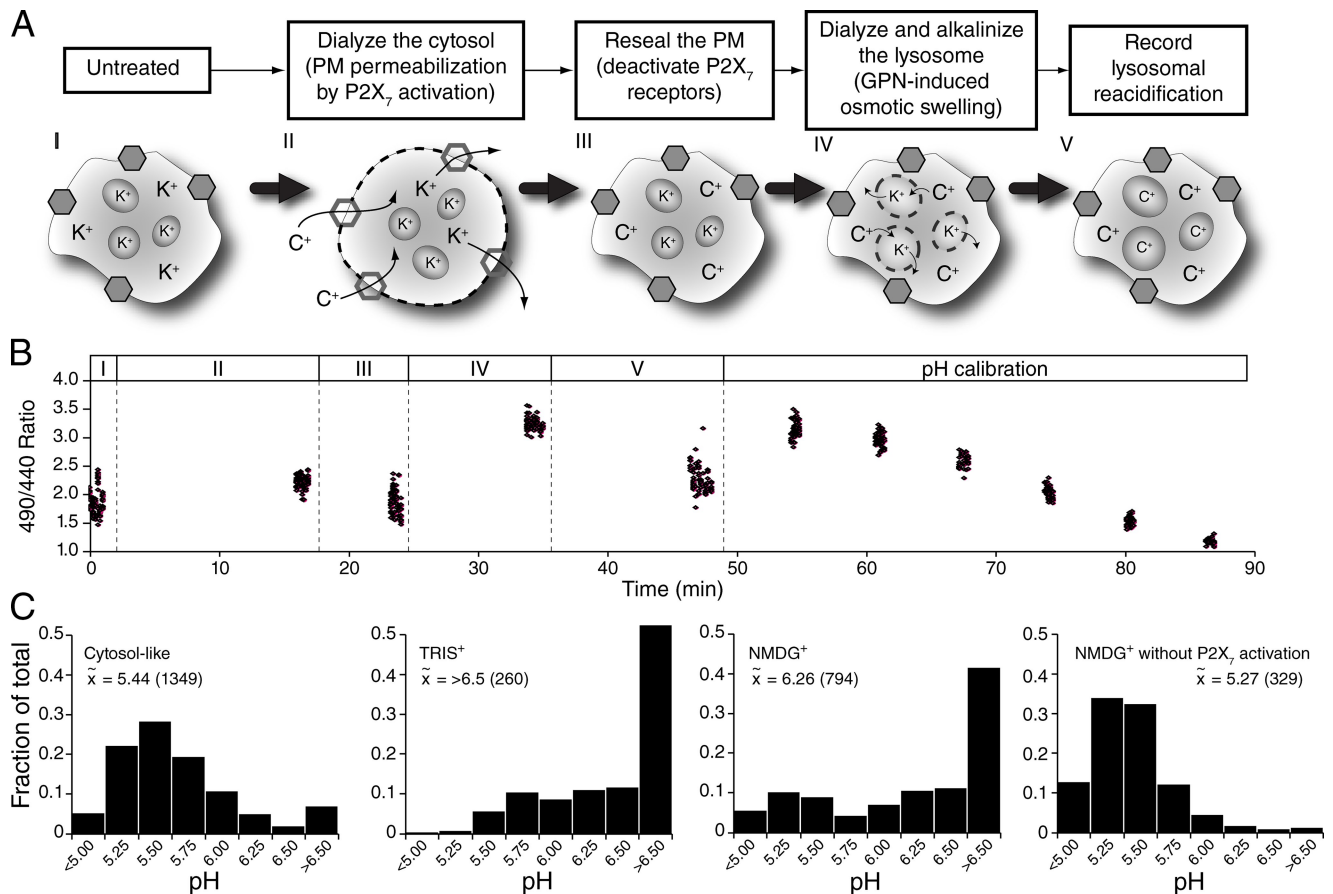
Figure 7. **Role of lysosomal cations in lysosome re-acidification after GPN-induced alkalinization.** (A) Schematic of the experimental protocol used to dialyze and transiently alkalinize lysosomes. After baseline pH measurements in RAW macrophages (step I), the cytosol was dialyzed by selectively permeabilizing the plasma membrane through the activation of resident P2X[7] receptors in the presence of cation substitution buffers (step II). Removal of the P2X[7] agonists and the addition of divalent cations resealed the plasma membrane (step III). The lysosomes were then dialyzed and alkalinized by GPN-induced osmotic swelling (step IV). The lysosomes were next allowed to re-acidify after removal of GPN (step V). An in situ calibration was performed at the end of each experiment (not illustrated). (B) Determinations of fluorescence ratio (proportional to pH) of a representative control experiment where cells were dialyzed with a cytosol-like solution. Each data point represents the ratio data from an individual region of interest. The steps indicated by Roman numerals refer to the protocol schematic of panel A. (C) Histograms of pooled lysosome pH determinations after recovery from the GPN treatment (step V of the illustrated protocol). The median pH of the lysosomes after the re-acidification period is given in the figure along with the total number of lysosomes used to compile the histograms. From left to right: cells dialyzed in cytosol-like (K$^+$-rich), Tris-substituted, or NMDG$^+$-substituted medium. The rightmost histogram shows cells that were incubated with NMDG$^+$-substituted medium but were not permeabilized. The histograms show collated data from nine, three, six, and two separate experiments, respectively.

normal lysosomal re-acidification was observed (median pH = 5.27; Fig. 7 C). When choline was used for dialysis, an intermediate level of re-acidification was observed (Fig. S3, D and E). Together, these observations indicate that, despite the presence of cytosolic Cl$^-$, small inorganic cations are required for proper acidification, suggesting that in lysosomes a cation counterflux can neutralize the electrogenicity of the V-ATPase.

A second, independent approach was used to validate the existence of a cation conductance in the lysosomal membrane. Conductive permeability was assessed by measuring the rate of dissipation of the lysosomal acidification upon treatment with FCCP. Because this protonophore is rheogenic, a counter-ion is required to support measurable net outward movement of H$^+$ from the lysosomes (Fig. 8 B). We determined the rate of alkalinization induced by FCCP after dialysis of the cytosol with solutions containing K$^+$, the predominant cytosolic cation, or NMDG$^+$, a large poorly permeant substituent (see Fig. 8 A for the experimental protocol). To gain insight into the identity of the monovalent

cationic counter-ion(s) that can support proton flux, we also compared Na$^+$, the predominant extracellular cation, with K$^+$. In the presence of cytosolic K$^+$ the lysosomes alkalinized rapidly, whereas the initial rate of alkalinization was considerably slower when using NMDG$^+$ (P < 0.05; Fig. 8, B and C). Na$^+$, on the other hand, was able to sustain an alkalinization rate comparable to that of K$^+$ (P > 0.05; Fig. 8, B and C). The above findings imply that counter-ion permeability can limit the flow of H$^+$ through the protonophore and, importantly, confirm the existence of sizable K$^+$ and Na$^+$ conductances in the lysosomal membrane.

Discussion

By developing new protocols to reversibly permeabilize the plasmalemma and the lysosomal membrane we were able to separately dialyze the cytosol and the lysosomal lumen to analyze the ionic dependence of acidification in situ. The primary finding of this study is that lysosomal luminal cations
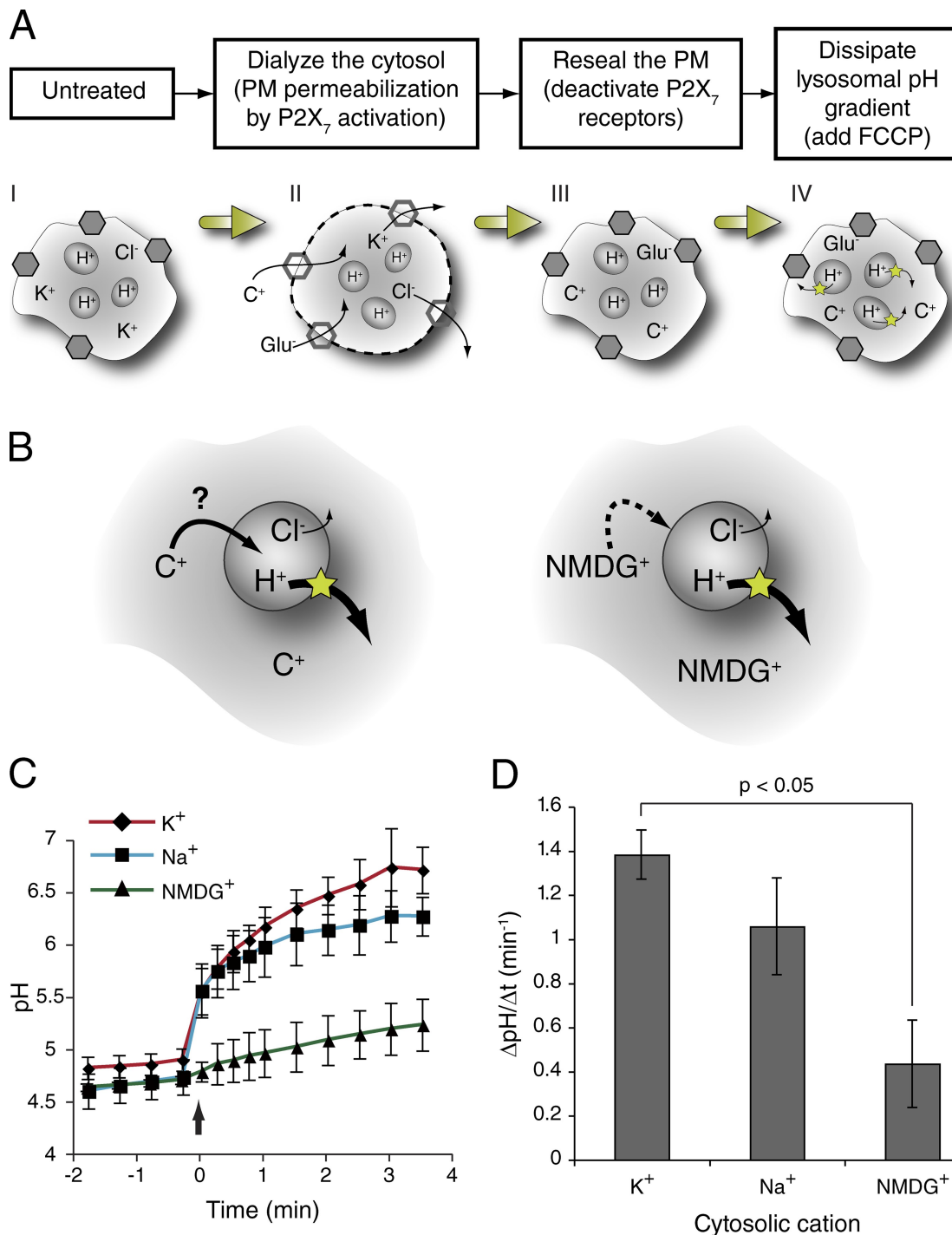
Figure 8. **Cytosolic cations support protonophore-induced lysosome alkalinization.** (A) Schematic representation of the experimental protocol used to dialyze and alkalinize the lysosomes. After baseline pH measurements (step I), the cytosol was dialyzed by selectively permeabilizing the plasma membrane through activation of P2X₇ receptors in the presence of suitable buffers (step II). Removal of the P2X₇ agonists and the addition of divalent cations resealed the plasma membrane (step III). The lysosomes were then alkalinized by FCCP treatment (step IV). (B) Proton efflux from lysosomes requires either the parallel efflux of an anion or the influx of a cation. When protonophore (green star) is added, counter-ions must move across the lysosome membrane to prevent membrane potential buildup. Before addition of the protonophore, the cytosol was dialyzed in the presence of either K⁺, Na⁺ (left) or NMDG⁺ (right), a relatively impermeant cation. If a K⁺ and/or Na⁺ conductance exists, NMDG⁺ will impair lysosome alkalinization, as it cannot be effectively transported into the lysosome lumen to dissipate the voltage. (C) Lysosome alkalinization in cells dialyzed with K⁺-rich (diamond), Na⁺-rich (squares), or NMDG⁺-rich solution (triangles). The time course of the change in pH after FCCP addition (arrow) is illustrated for representative experiments (means ± SD). (D) The rate of pH dissipation over the first minute of FCCP-induced alkalinization for the three different cations.

can function as the counter-ions that enable lysosomal acidification by dissipating the membrane potential generated by the V-ATPase.

We found that, in otherwise untreated cells, the lysosomes were able to re-acidify fully after a transient protonophore-induced alkalinization. Strikingly, the re-acidification was equally

rapid and complete in cells where the cytosolic Cl⁻ had been replaced with large organic anions such as gluconate and $MeSO_3^-$. Because these are negligibly permeable through most Cl⁻ conductive pathways, including CLC chloride transporters and CFTR channels (Linsdell et al., 1997; Jentsch, 2008), we inferred that cytosolic anions are not absolutely essential for lysosome acidification. That cytosolic anions are dispensable was corroborated by measuring re-acidification in a cell-free preparation of isolated lysosomes in the absence of Cl⁻ (Fig. 4). In both types of experiments, protonophores were used to dissipate the preexisting pH gradients, and this was followed by protonophore removal to reinitiate acidification. It is most likely that removal of the protonophore was not complete, which would result in underestimation of the rate of the V-ATPase due to futile cycles of proton pumping and leakage. Nevertheless, the measured acidification required net transport of protons with concomitant transport of a counter-ion other than chloride. This conclusion differs from those reached by others, but differences in the experimental design may account for the apparent discrepancies. Moreover, our data do not negate the existence of a parallel anion conductance. Indeed, we were able to confirm that, when cations are removed from the lumen of the lysosomes, a Cl⁻-dependent acidification is revealed (Fig. 4 C). Thus, lysosomal proton pumping can be supported by either an influx of Cl⁻ or by the exit of luminal cations.

In an important study, acidification was studied in situ in macrophages and found to require anion transport via CFTR (Di et al., 2006). More recently, defective lysosomal acidification was also invoked as the mechanism underlying ceramide accumulation in CF lysosomes (Teichgräber et al., 2008). Yet the conclusions reached by Di et al. (2006) regarding the role of CFTR in lysosomes are not universally accepted. The observations of Haggie and Verkman (2007) and Barriere et al. (2009) failed to confirm the involvement of CFTR in acidification, as did ours. We found that pharmacological inhibition of CFTR channel activity did not perturb lysosome pH and that primary alveolar macrophages lacking functional CFTR had no measurable impairment in lysosomal acidification. In fact, it is not clear whether CFTR would be operational at the extremely acidic pH that prevails in the lysosomal lumen. In BHK cells stably expressing CFTR on their plasma membrane the anion flux induced by elevation of cAMP was acutely inhibited when the pH of the bathing medium, topologically equivalent to the lysosome lumen, was reduced to 4.5 to mimic the lysosomal pH (Fig. S4). Taken together, the available data do not convincingly support a role for CFTR in lysosomal counter-ion conductance and defects in lysosomal acidification cannot fully explain the impaired microbicidal capacity in CF.

Similarly, the Cl⁻/H⁺ antiporter ClC-7 has also been implicated as the counter-ion conductance in lysosomal acidification (Kornak et al., 2001; Graves et al., 2008). As proposed for other family members, uptake of Cl⁻ via ClC-7 could in principle serve as a neutralizing counter-ion to H⁺ pumping, though the process would be inefficient (three H⁺ pumped for every two accumulated if the stoichiometry of exchange is 2:1). However, lysosomal pH appears to be normal in macrophages from mice lacking ClC-7 (Fig. 2), as described previously for other cells

(Kornak et al., 2001; Kasper et al., 2005; Lange et al., 2006), implying that alternative counter-ion pathways exist in lysosomes. The experiments of Graves et al. (2008), which assigned to ClC-7 an essential role in lysosomal acidification, suffer from apparent methodological limitations that may explain the discrepancy with our results and those of Kasper et al. (2005) and Lange et al. (2006). In brief, Graves et al. (2008) used an acidotropic dye, LysoTracker, to estimate lysosomal pH. Accumulation of Lyso-Tracker is an indirect and qualitative assay of pH, which is affected by the number and size of acidic vesicles, parameters that were not determined by Graves et al. (2008). In addition, their evidence for a role for ClC-7 in lysosome pH regulation relied on incomplete knockdown of the antiporter using a single siRNA. The interpretation of their data are further complicated by the disconcerting fact that their control siRNA treatment significantly increased LysoTracker fluorescence, even though it decreased ClC-7 expression to some extent. Thus, rather than having no effect, the control treatment seemed to acidify or enlarge lysosomes. Considering these shortcomings, the results obtained with ratiometric fluorescence measurements in $Clcn7^{-/-}$ cells appear more reliable. Whether in knock-out or knock-down cells other vesicular ClC proteins can partially substitute for ClC-7 remains to be determined.

That lysosomes could acidify in the absence of permeable anions prompted us to consider whether lysosomal cations were capable of sustaining proton translocation by the V-ATPase. Because, to the best of our knowledge, the free concentration of inorganic cations in lysosomes had not been reported, the presence of potential luminal counter-ions had to be validated first. Our null-point determinations of Na⁺ and K⁺ activity indicated that inorganic cations are sufficiently abundant to sustain the acidification of lysosomes. It must be borne in mind that, in addition, inorganic cations taken up by fluid-phase endocytosis are delivered continuously to lysosomes, providing a continued source of potential counter-ions. More importantly, ion replacement experiments demonstrated that monovalent inorganic cations support the acidification process. This conclusion is not unprecedented; some in vitro studies had suggested that K⁺ plays a more prominent role in facilitating lysosome acidification than does Cl⁻ (Moriyama, 1988; Van Dyke, 1993). It is noteworthy also that lysosomes store significant amounts of Ca^{2+} (Haller et al., 1996a; Christensen et al., 2002) and this divalent cation could in principle also contribute to neutralize H⁺ entry. However, we have thus far failed to confirm the participation of calcium: omission of calcium from the resealing solution in experiments like those in Fig. 3 had no discernible effect on the rate of re-acidification, and elevation of cytosolic calcium by treatment of cells with thapsigargin had no effect on lysosomal pH (Fig. S5).

It is interesting to speculate why lysosomes may use cations in addition to or instead of anions as counter-ions for acidification. Although anion influx and cation efflux would equally neutralize the charge accrued by proton translocation, the osmotic consequences of these processes are diametrically opposed. The uptake of an anion in parallel with each H⁺ results in a net osmotic gain. The osmotic implications of counter-ion transport are best appreciated when considering that the intrinsic

buffering power of lysosomes is comparatively high (61.5 ± 2.3 mM/pH at steady state in macrophages), likely due to their high protein content. Using the empirically measured intrinsic lysosomal buffering power, integrated over the pH 4.5–6.5 range (Fig. S5 D), full acidification of the lysosome would require the parallel transport of ≥108 mmol of counter-ions per liter of lysosomal volume. This gain in anionic osmolytes would cause considerable swelling and possibly lysis of the lysosomes, which are water permeable and susceptible to osmotically induced rupture, as revealed by the experiments using GPN. The ensuing collapse of the pH gradient and the release of degradative enzymes would obviously have a detrimental effect on the cell. By contrast, use of cations as counter-ions during acidification would guard against volume expansion. Instead, because incoming protons are largely scavenged by the luminal buffer, the loss of cations would result in lysosomal shrinking. By combining the use of cations and anions as counter-ions to protons, the lysosomes may be able to maintain their osmolarity and volume during the course of acidification.

To our knowledge, few specific cation channels or electrogenic transporters have been shown conclusively to function in the lysosomal membrane. Proteomic approaches are beginning to probe the protein landscape of the lysosomal membrane (Schröder et al., 2007) and, as more extensive lists are developed and consolidated, candidate conductive pathways will be identified. Their ability to function in the unusual environment of the lysosome and their role in lysosome acidification must then be tested.

Materials and methods

Materials
CFTR$_{INH}$-172 was purchased from EMD. Sulforhodamine 101, LysoTracker Red, Oregon Green 514-dextran, fluorescein-dextran, and rhodamine B–dextran were from Invitrogen. All dextrans were of 10,000 MW. Unless specified otherwise, all other reagents were from Sigma-Aldrich. Phosphate-buffered saline (PBS; 154 mM NaCl, 1.1 mM KH$_2$PO$_4$, and 5.6 mM Na$_2$HPO$_4$) was purchased from Wisent.

Cell lines and tissue culture
RAW264.7 (number TIB-71) and J774 (number TIB-67) murine macrophage cell lines were obtained from the American Type Culture Collection (Rockville, MD) and grown at 37°C under 5% CO$_2$ in DME supplemented with 5% fetal bovine serum (FBS; Wisent).

Bi-transgenic cftr-null mutant (cftr$^{-/-}$) mice, expressing human CFTR in the gut under the control of the rat fatty acid–binding protein (FABP) promoter (strain Cftr^{tm1Unc}-Tg$^{(FABPCFTR)}$), and their littermate controls (cftr$^{+/+}$), were obtained from the Cystic Fibrosis Animal Core at Case Western Reserve University (Cleveland, OH). RT-PCR determinations using the primers 5′-TAAACCTACCAAGTCAACCA-3′ forward, 5′-AATTCCATGAGCAAAT-GTC-3′ reverse, failed to detect expression of the human transgene in the alveolar macrophages, whereas expression was clearly detectable in parallel samples of human airway epithelial cells (not illustrated). The Clcn7$^{-/-}$ mice, on a C57BL/6-129SV mixed background, as well as the murine adult fibroblasts, were described previously (Kornak et al., 2001). All animal protocols were approved by the animal care committee of the Hospital for Sick Children or the competent authorities of the city-state of Berlin.

To isolate alveolar macrophages, the mice were sacrificed and bronchoalveolar lavage performed. For each lavage, 1 ml of cold PBS supplemented with 1 mM CaCl$_2$ and 1 mM MgCl$_2$ was instilled into the lungs by tracheal cannulation. The lavage was repeated three times to collect between 2 and 3 ml of fluid. The collected cells from each mouse were cultured on glass coverslips at 37°C under 5% CO$_2$ in RPMI 1640 medium supplemented with 10% FBS and a penicillin, streptomycin, and amphotericin B cocktail. Alveolar macrophages were used within 3 d of harvesting.

Immunofluorescence microscopy
For immunostaining, macrophages were fixed with 4% PFA in PBS for 15 min, incubated with 30 mM glycine in PBS for 5 min and permeabilized with 0.05% saponin in PBS for 10 min. Both primary and Alexa Fluor–coupled secondary (Invitrogen) antibodies were applied in PBS/0.05% saponin supplemented with 3% BSA. Primary antibodies used were rat anti-mLamp1 (BD), rat anti-mF4/80 (Cedarlane), and rabbit anti–ClC-7 (Kornak et al., 2001). Images were acquired with a laser-scanning confocal microscope (model LSM510; Carl Zeiss, Inc.) equipped with a 63x 1.4 NA oil-immersion lens using the ZEN imaging software (Carl Zeiss, Inc.). Images were further processed using Photoshop (Adobe).

Lysosomal pH measurements
Lysosomal pH measurements were performed by ratiometric fluorescence imaging of a pH-sensitive fluorophore specifically targeted to the compartment of interest using a standard pulse-chase protocol. Cultured cells were plated on glass coverslips and grown overnight in the presence of 500 µg/ml of Oregon Green 514–conjugated dextran. The cells were then washed and the dextran chased to the lysosome by incubating the cells at 37°C for 1 h in the presence of serum followed by 1 h in serum-free medium before imaging. Where indicated, cells were incubated with the indicated pharmacological agent during the hour in serum-free medium and then maintained in its presence for the duration of the experiment.

For imaging, coverslips were placed in a Leiden chamber maintained at 37°C and mounted on the stage of a microscope (model DM IRB; Leica). pH was measured by fluorescence ratiometric imaging using a filter wheel (Sutter Instrument Co.) to rapidly alternate between excitation filters. The cells were excited by light from an XFO X-Cite 120 lamp (XFO Life Sciences Group) transmitted alternately through 485 ± 10 nm and 438 ± 12 nm excitation filters and directed to the sample using a 505-nm dichroic mirror. The emitted light was filtered with a 535 ± 20 nm filter before being captured by a CCD camera (Cascade II; Photometrics). The filter wheel and camera were under the control of MetaFluor software (MDS Analytical Technologies).

At the end of each experiment, an in situ calibration was performed. The cells were sequentially bathed in isotonic K$^+$ solutions (145 mM KCl, 10 mM glucose, 1 mM MgCl$_2$, and 20 mM of either Hepes, MES, or acetate) buffered to pH ranging from 4.0 to 6.5 and containing 10 µg/ml of nigericin. Images were acquired 5 min after the addition of each solution to ensure equilibration of pH across compartments. The resulting fluorescence intensity ratio (490 nm/440 nm) data as a function of pH were fit to a Boltzmann sigmoid and used to interpolate pH values from the experimental ratio data. By bathing the cells in 145 mM KCl, the K$^+$ concentration gradient between the medium and the cytosol is virtually eliminated and the ionophore drives the cytosolic pH to that of the bathing medium. Nigericin also inserts into and functions within the lysosomal membrane. To fully equilibrate the lysosomal pH with that of the cytosol (and thus the bathing medium), we assume that there is a negligible K$^+$ concentration gradient across the lysosome membrane. Based on our null-point titration K$^+$ determinations (Fig. 5) at steady state, there is approximately a threefold concentration difference. Were there no buffering power in the lysosome, this gradient would affect the pH measurement by ∼0.5 (log 3) pH units. However, this error is mitigated by the lysosomal buffering power measured at 60–80 mM in the pH 4.5–5.5 range, which decreases the discrepancy to ≤0.13 pH units, and by the existence of K$^+$ permeation pathways within the lysosomal membrane that promote equilibration between the lysosomal and cytosolic K$^+$.

The intrinsic lysosomal buffering power was determined by measuring the change in pH induced by graded pulses of weak electrolytes and calculated as described by Roos and Boron (1981). To estimate the buffering power as a function of pH, the V-ATPase was inhibited by addition of 500 nM CcA to slowly dissipate the luminal acidification. When the desired pH was attained, NH$_4$Cl was added to the bathing medium and the magnitude of the sudden alkalinization was recorded. In this manner, we calculated the buffering power over 0.5 pH unit intervals in the range of pH 4.5–6.5.

Lysosome pH measurements in Clcn7$^{-/-}$ mice
Alveolar macrophages from ClC-7 knockout mice (Kornak et al., 2001) 3.5–5 wk of age were harvested as above. The cells were plated on glass-bottom live-cell dishes (MatTek) and pH measurements were performed after 2 d. Lysosomes were loaded with 0.5 mg/ml Oregon Green 488–dextran (Invitrogen) in RPMI supplemented with 10% FBS for at least 2 h followed by a 2-h chase. In experiments investigating the effect of CFTR$_{INH}$-172, the drug (10 µM) was added to the medium 1 h before measurements. Images were acquired at 37°C using a microscope (Axiovert 200; Carl Zeiss, Inc.)

equipped with a 100x 1.30 NA oil-immersion lens, and with excitation at 440 and 488 nm delivered by a Polychrom II monochromator system (TILL Photonics). The emitted light was selected with a 535 ± 20 nm filter and captured with a Sensicam CCD camera. For each animal, at least 10 different cells with at least 10 single lysosomes each were measured in 150 mM NaCl, 1 mM $MgCl_2$, 2 mM $CaCl_2$, 10 mM glucose, and 10 mM Hepes, pH 7.4. Calibration was as above, but using both nigericin and monensin (10 µM each). Image acquisition and analysis were performed using TILL-vision software (TILL Photonics). Data were exported to Excel (Microsoft) for further analysis and display.

Ion substitution and re-acidification protocols

Lysosomes in RAW macrophages were loaded with Oregon Green 514–dextran and baseline pH recorded. The cytosol was subsequently dialyzed by incubating the cells in a dialysis medium containing 50 mM KCl, 90 mM K gluconate, 20 mM Hepes, 10 mM glucose, 1 mM EDTA, 1 mg/ml dextran (MW 1,500), 2.5 mM Na_2ATP, and 100 µM bzATP to activate plasmalemmal $P2X_7$ receptors. Where specified, Cl^- was isoosmotically replaced with either gluconate or $MeSO_3^-$. In all cases, the dialysis medium also contained 500 nM FCCP to alkalinize the lysosomes. After 15 min of cytosol dialysis and lysosome alkalinization, re-acidification was initiated by washing the cells threefold with dialysis buffer supplemented with 3 mM $MgCl_2$ and 1% albumin but without $P2X_7$ agonists and protonophore. The inclusion of 2 mM $CaCl_2$ in the re-acidification medium did not impact on the rate or extent of lysosome re-acidification (Fig. S5 A). An in situ calibration concluded each experiment. A single field was monitored throughout the protocol.

A derivative of the above protocol was used to examine the role of lysosomal cations in lysosomal re-acidification. After baseline lysosome pH measurements in the RAW cells, the cytosol was dialyzed by incubation with a $P2X_7$ activation solution containing 90 mM K gluconate, 50 mM KCl, 20 mM Hepes, 10 mM glucose, 1 mM EDTA, 1 mg/ml dextran (MW 1,500), 2.5 mM Na_2ATP, and 100 µM bzATP for 15 min. Where specified, K^+ was replaced with $NMDG^+$, choline, or Tris; 50 mM Cl^- was used throughout to approximate cytosolic Cl^- levels. For the remainder of the experiment, the cells were maintained in a deactivation solution similar to the dialysis medium but without the $P2X_7$ agonists and supplemented with 1 mM $CaCl_2$ and 1 mM $MgCl_2$. The cells were allowed 5 min to recover before initiating lysosomal dialysis and alkalinization through the addition of 200 µM GPN to the bathing medium. After 10 min the cells were washed to remove GPN and given a further 10 min to recover. The protocol concluded with an in situ calibration. At the end of each step of the protocol, images from 5 to 15 fields were acquired.

The role for cations as possible counter-ions for lysosome H^+ transport was also examined by measuring protonophore-induced alkalinization in the presence and absence of permeant cytosolic cations. The lysosomes of RAW macrophages were first loaded with Oregon Green 514–dextran by the pulse-chase protocol described above, followed by dialysis of the macrophage cytosol by incubation with a $P2X_7$ activation solution containing 140 mM K gluconate, 20 mM Hepes, 10 mM glucose, 1 mM EDTA, 1 mg/ml dextran (MW 1,500), and 100 µM bzATP for 15 min. Where indicated, K^+ was replaced with an equivalent amount of $NMDG^+$. The cells were then maintained in a deactivation solution similar to the dialysis medium but supplemented with 1 mM $MgCl_2$ and devoid of $P2X_7$ agonists. After 5 min of recovery, 1 µM FCCP was added to the bathing medium and the rate of lysosome alkalinization was monitored. A single field of cells was imaged throughout in each experiment.

Re-acidification of isolated lysosomes

The lysosomes of RAW macrophages were loaded with Oregon Green–dextran using the pulse-chase protocol described above. The cells were washed with either a Cl^--containing (90 mM K gluconate, 50 mM KCl, 1mM EGTA, 20 mM Hepes, 50 mM sucrose, and protease inhibitor cocktail, pH 7.3) or Cl^--free solution (as above except with all the chloride replaced with gluconate) before treatment with 1 µM FCCP for 15 min in order to completely dissipate the lysosomal pH gradient. Without the ionophore the lysosomes remained acidic, precluding assessment of the rate of acidification. The FCCP-treated cells were scraped into 1.5 ml of the appropriate buffer and homogenized in a Dounce homogenizer. To prevent lysosomal re-acidification during the course of fractionation, the cells and homogenate were maintained in the continued presence of FCCP at 4°C until the final wash of the isolated organelles. To remove nuclei and unbroken cells the homogenate was centrifuged at 10,000 rpm for 15 s. The endomembranes in the recovered supernatant were next sedimented by centrifugation at 13,200 rpm at 4°C for 20 min, and then resuspended in 1 ml of the appropriate buffer prewarmed to 37°C, without FCCP and supplemented with 1% albumin to scavenge remaining ionophore. The protocol

duration was minimized to ensure that the isolated organelles maintained their structural integrity. Sedimentation experiments showed that, under these conditions, less than 2% of the fluorescence was extralysosomal at the time of the measurements.

The lysosome-enriched preparation was maintained at 37°C and its fluorescence monitored using a fluorescence spectrophotometer (model F-2500; Hitachi) by exciting the sample at 490 ± 5 nm and recording the emitted light at 520 ± 5 nm. A baseline pH measurement was performed in every experiment; the average starting lysosomal pH was 6.7. After the baseline determination, 5 mM Mg (either as the Cl^- or sulfate salt, as appropriate) and 5 mM ATP was added to the suspension, while continually monitoring fluorescence. Where indicated, 500 nM CcA was added along with the ATP to the suspension. At the end of the acidification, nigericin (10 µg/ml) was added to the sample to alkalinize the suspended lysosomes and ensure that they maintained their integrity over the course of the experiment.

A similar protocol was used to demonstrate the presence of an electrogenic Cl^- conductance in the lysosome membrane. To minimize the contribution of any cation conductance(s), we first depleted lysosomal cations by incubating the intact cells in an $NMDG^+$-based medium (90 mM NMDG gluconate, 50 mM NMDG Cl, 20 mM Hepes, 10 mM glucose, 1 mM $MgCl_2$, and 1 mM $CaCl_2$) for 1 h with frequent washes. The remainder of the experiment was similarly performed in solutions devoid of small, inorganic cations. The cells were then treated with FCCP for 15 min to ensure that the lysosome pH gradient was dissipated. Lysosomes, preloaded with FITC-dextran as above, were then harvested in a sucrose-based medium (350 mM sucrose, 1mM EGTA, 20 mM Hepes, and protease inhibitor cocktail, pH 7.3). Where specified, this medium was supplemented with 50 mM chloride (as the NMDG salt). In these instances the sucrose content was decreased accordingly to maintain osmolarity.

Null-point titration determinations of lysosomal K^+ and Na^+

The ionophores used for the null-point titration experiments catalyze the stoichiometric and electroneutral exchange of protons for alkali cations. In the case of nigericin, which is highly selective for K^+, no net movement of protons across the membrane—and thus no pH change—will be induced by addition of the ionophore when

$$\frac{H_l}{H_c} = \frac{K_l}{K_c},$$

where H_l is the lysosomal proton activity, H_c is the cytosolic proton activity, K_l is the lysosomal potassium activity, and K_c is the cytosolic potassium activity. From this "null-point" the lysosomal potassium activity can be calculated as

$$K_l = K_c \times 10^{(pH_c - pH_l)}.$$

Monensin prefers Na^+, but significant transport of K^+ also occurs. In this case the null-point is defined by:

$$\frac{H_l}{H_c} = \frac{Na_l + \left(\frac{P_K K_{Na}}{P_{Na} K_K}\right) K_l}{Na_c + \left(\frac{P_K K_{Na}}{P_{Na} K_K}\right) K_c},$$

where H_l, H_c, K_l, and K_c are as defined above, Na_l is the lysosomal sodium activity, Na_c is the cytosolic sodium activity, P_K and P_{Na} are the potassium- and sodium-ionophore complex translocation rates, respectively, and κ_K and κ_{Na} are, respectively, the potassium and sodium dissociation rates from the ionophore.

From the above relationship we obtain

$$Na_l = \left[Na_c + \frac{1}{P} K_c\right] \times 10^{(pH_c - pH_l)} - \frac{1}{P} K_l,$$

where

$$\frac{1}{P} = \left(\frac{P_K K_{Na}}{P_{Na} K_K}\right).$$

Our calculations use a selectivity coefficient P of 25, in accordance with published estimates (Prabhananda and Kombrabail, 1992; Nachliel et al., 1996; Rochdi et al., 1996).

To carry out determinations of lysosomal K^+ by null-point titration, RAW264.7 cells were plated on glass coverslips and their lysosomes loaded with fluorescein-labeled dextran using the pulse-chase protocol described above. The cytosolic ion composition was manipulated by incubating the cells for 15 min in titration buffer (10 mM NaCl, 20 mM KCl, 20 mM NMDG Cl, 90 mM NMDG gluconate, 10 mM glucose, 20 mM MES, and 1 mg/ml of 1,500 MW dextran, set to pH 6.5 or 7.3, as indicated, with NaOH) containing 100 µM bzATP and 2 mM Na_2ATP to stimulate $P2X_7$ receptors. The solution was replaced with titration buffer without the $P2X_7$ agonists and containing various concentrations of trimethylamine (TMA) to alkalinize the lysosome, plus 1 µM CcA to inhibit the V-ATPase. After 2–4 min, nigericin (10 µg/ml) was added to the medium. An in situ calibration was performed at the end of each experiment. A single field was monitored by ratiometric imaging at every step of the protocol. Na^+ determinations were similar, except the titration buffer consisted of 10 mM NaCl, 40 mM KCl, 10 mM K gluconate, 80 NMDG gluconate, 10 mM glucose, 20 mM MES, and 1 mg/ml of 1,500 MW dextran, set to pH 6.5 with Tris, and monensin (20 µg/ml) was used instead of nigericin.

Colorimetric determination of intracellular Cl^-

The colorimetric chloride determination was adapted from Zall et al. (1956). Cells were either left untreated or had their cytosol dialyzed by incubation in a nitrate-based $P2X_7$ receptor activation solution (140 KNO_3, 20 mM Hepes, 10 mM glucose, 1 mM EDTA, 2.5 mM Na_2ATP, 100 µM bzATP, and 1 mg/ml dextran) for 15 min. They were subsequently washed thoroughly with cold $NaNO_3$ medium (130 mM $NaNO_3$, 3 mM KNO_3, 1 $Mg(NO_3)_2$, 1 $Ca(NO_3)_2$, 10 mM glucose, and 20 mM Hepes, pH 7.4), then lysed in 1 mM nitric acid. After centrifugation, the supernatant was collected and mixed with an equal volume of the photometric determination solution (1 part 0.417% mercuric thiocyanate in methanol, 1 part 20.2% ferric nitrate solution, and 13 parts water). The ferric nitrate was made by dissolving 20.2 g of ferric nitrate in 31 ml of 4 N HNO_3, which was brought to a final volume of 100 ml with distilled water. The absorbance at 480 nm of the experimental samples and Cl^- standards was determined using a VERSAmax microplate reader (MDS Analytical Technologies). In parallel experiments, cells were incubated in the nitrate-based, chloride-free medium for 1.5 h with frequent washes, and similarly prepared. The signal from these samples consists of nonexchangeable chloride and nonspecific background of the colorimetric reaction, which were subtracted from all experimental samples. Cell number and volume were determined in parallel using the Coulter-Channelyzer in order to calculate intracellular Cl^- concentrations.

Data analysis and statistics

Measurements of lysosome re-acidification after protonophore-induced alkalinization were fit with a single exponential of the form $y = A * \exp(-K x) + B$ to calculate the half-life of the pH decay ($\tau = 0.69/K$) reported in Table I. Null-point titration data were fit using least-squares linear regression to determine the x-intercept.

Data are reported as representative traces or mean ± SE for the indicated number of experiments. The statistical significance of differences between multiple groups was determined using analysis of variance (ANOVA) with Dunnett's multiple comparison test for pairwise comparisons with control data. P-values <0.05 were considered statistically significant. Statistical analyses were performed using either SAS or Prism 4 by Graph-Pad Software, Inc.

Online supplemental material

Fig. S1 shows the colocalization of ClC-7 with LAMP-1 in alveolar macrophages. Fig. S2 shows validation of the effectiveness of the cytosolic dialysis accomplished by activation of $P2X_7$ and a comparison of two independent null-point titrations of lysosomal K^+ content. Fig. S3 illustrates the occurrence of lysosome re-acidification after luminal cation dialysis. Fig. S4 shows that cAMP-dependent iodide efflux was readily detectable in CFTR-expressing BHK cells but not in their untransfected counterparts, and also illustrates the effect of extracellular acidification on CFTR function. Fig. S5 analyses the effect of calcium on lysosomal pH and shows the pH dependence of the lysosomal buffering power. Online supplemental material is available at http://www.jcb.org/cgi/content/full/jcb.200911083/DC1.

References

Barriere, H., M. Bagdany, F. Bossard, T. Okiyoneda, G. Wojewodka, D. Gruenert, D. Radzioch, and G.L. Lukacs. 2009. Revisiting the role of cystic fibrosis transmembrane conductance regulator and counterion permeability in the pH regulation of endocytic organelles. *Mol. Biol. Cell.* 20:3125–3141. doi:10.1091/mbc.E09-01-0061

Berg, T.O., E. Strømhaug, T. Løvdal, O. Seglen, and T. Berg. 1994. Use of glycyl-L-phenylalanine 2-naphthylamide, a lysosome-disrupting cathepsin C substrate, to distinguish between lysosomes and prelysosomal endocytic vacuoles. *Biochem. J.* 300:229–236.

Christensen, K.A., J.T. Myers, and J.A. Swanson. 2002. pH-dependent regulation of lysosomal calcium in macrophages. *J. Cell Sci.* 115:599–607.

Di, A., M.E. Brown, L.V. Deriy, C. Li, F.L. Szeto, Y. Chen, P. Huang, J. Tong, A.P. Naren, V. Bindokas, et al. 2006. CFTR regulates phagosome acidification in macrophages and alters bactericidal activity. *Nat. Cell Biol.* 8:933–944. doi:10.1038/ncb1456

Forgac, M. 2007. Vacuolar ATPases: rotary proton pumps in physiology and pathophysiology. *Nat. Rev. Mol. Cell Biol.* 8:917–929. doi:10.1038/nrm2272

Graves, A.R., P.K. Curran, C.L. Smith, and J.A. Mindell. 2008. The Cl-/H+ antiporter ClC-7 is the primary chloride permeation pathway in lysosomes. *Nature.* 453:788–792. doi:10.1038/nature06907

Günther, W., A. Lüchow, F. Cluzeaud, A. Vandewalle, and T.J. Jentsch. 1998. ClC-5, the chloride channel mutated in Dent's disease, colocalizes with the proton pump in endocytotically active kidney cells. *Proc. Natl. Acad. Sci. USA.* 95:8075–8080. doi:10.1073/pnas.95.14.8075

Günther, W., N. Piwon, and T.J. Jentsch. 2003. The ClC-5 chloride channel knock-out mouse - an animal model for Dent's disease. *Pflügers Arch.* 445:456–462.

Haggie, P.M., and A.S. Verkman. 2007. Cystic fibrosis transmembrane conductance regulator-independent phagosomal acidification in macrophages. *J. Biol. Chem.* 282:31422–31428. doi:10.1074/jbc.M705296200

Haller, T., P. Dietl, P. Deetjen, and H. Völkl. 1996a. The lysosomal compartment as intracellular calcium store in MDCK cells: a possible involvement in InsP3-mediated Ca2+ release. *Cell Calcium.* 19:157–165. doi:10.1016/S0143-4160(96)90084-6

Haller, T., H. Völkl, P. Deetjen, and P. Dietl. 1996b. The lysosomal Ca2+ pool in MDCK cells can be released by ins(1,4,5)P3-dependent hormones or thapsigargin but does not activate store-operated Ca2+ entry. *Biochem. J.* 319:909–911.

Hara-Chikuma, M., Y. Wang, S.E. Guggino, W.B. Guggino, and A.S. Verkman. 2005a. Impaired acidification in early endosomes of ClC-5 deficient proximal tubule. *Biochem. Biophys. Res. Commun.* 329:941–946. doi:10.1016/j.bbrc.2005.02.060

Hara-Chikuma, M., B. Yang, N.D. Sonawane, S. Sasaki, S. Uchida, and A.S. Verkman. 2005b. ClC-3 chloride channels facilitate endosomal acidification and chloride accumulation. *J. Biol. Chem.* 280:1241–1247. doi:10.1074/jbc.M407030200

Jadot, M., C. Colmant, S. Wattiaux-De Coninck, and R. Wattiaux. 1984. Intralysosomal hydrolysis of glycyl-L-phenylalanine 2-naphthylamide. *Biochem. J.* 219:965–970.

Jentsch, T.J. 2008. CLC chloride channels and transporters: from genes to protein structure, pathology and physiology. *Crit. Rev. Biochem. Mol. Biol.* 43:3–36. doi:10.1080/10409230701829110

Kasper, D., R. Planells-Cases, J.C. Fuhrmann, O. Scheel, O. Zeitz, K. Ruether, A. Schmitt, M. Poët, R. Steinfeld, M. Schweizer, et al. 2005. Loss of the chloride channel ClC-7 leads to lysosomal storage disease and neurodegeneration. *EMBO J.* 24:1079–1091. doi:10.1038/sj.emboj.7600576

Kornak, U., D. Kasper, M.R. Bösl, E. Kaiser, M. Schweizer, A. Schulz, W. Friedrich, G. Delling, and T.J. Jentsch. 2001. Loss of the ClC-7 chloride channel leads to osteopetrosis in mice and man. *Cell.* 104:205–215. doi:10.1016/S0092-8674(01)00206-9

Lamothe, J., and M.A. Valvano. 2008. *Burkholderia cenocepacia*-induced delay of acidification and phagolysosomal fusion in cystic fibrosis

transmembrane conductance regulator (CFTR)-defective macrophages. *Microbiology.* 154:3825–3834. doi:10.1099/mic.0.2008/023200-0

Lange, P.F., L. Wartosch, T.J. Jentsch, and J.C. Fuhrmann. 2006. ClC-7 requires Ostm1 as a beta-subunit to support bone resorption and lysosomal function. *Nature.* 440:220–223. doi:10.1038/nature04535

Li, X., T. Wang, Z. Zhao, and S.A. Weinman. 2002. The ClC-3 chloride channel promotes acidification of lysosomes in CHO-K1 and Huh-7 cells. *Am. J. Physiol. Cell Physiol.* 282:C1483–C1491.

Linsdell, P., J.A. Tabcharani, J.M. Rommens, Y.X. Hou, X.B. Chang, L.C. Tsui, J.R. Riordan, and J.W. Hanrahan. 1997. Permeability of wild-type and mutant cystic fibrosis transmembrane conductance regulator chloride channels to polyatomic anions. *J. Gen. Physiol.* 110:355–364. doi:10.1085/jgp.110.4.355

Ma, T., J.R. Thiagarajah, H. Yang, N.D. Sonawane, C. Folli, L.J. Galietta, and A.S. Verkman. 2002. Thiazolidinone CFTR inhibitor identified by high-throughput screening blocks cholera toxin-induced intestinal fluid secretion. *J. Clin. Invest.* 110:1651–1658.

McGuinness, L., S.J. Bardo, and N.J. Emptage. 2007. The lysosome or lysosome-related organelle may serve as a Ca2+ store in the boutons of hippocampal pyramidal cells. *Neuropharmacology.* 52:126–135. doi:10.1016/j.neuropharm.2006.07.029

Mohammad-Panah, R., R. Harrison, S. Dhani, C. Ackerley, L.J. Huan, Y. Wang, and C.E. Bear. 2003. The chloride channel ClC-4 contributes to endosomal acidification and trafficking. *J. Biol. Chem.* 278:29267–29277. doi:10.1074/jbc.M304357200

Moriyama, Y. 1988. Potassium ion dependent proton efflux and depolarization from spleen lysosomes. *Biochem. Biophys. Res. Commun.* 156:211–216. doi:10.1016/S0006-291X(88)80826-X

Nachliel, E., Y. Finkelstein, and M. Gutman. 1996. The mechanism of monensin-mediated cation exchange based on real time measurements. *Biochim. Biophys. Acta.* 1285:131–145. doi:10.1016/S0005-2736(96)00149-6

Pelegrin, P., and A. Surprenant. 2006. Pannexin-1 mediates large pore formation and interleukin-1beta release by the ATP-gated P2X7 receptor. *EMBO J.* 25:5071–5082. doi:10.1038/sj.emboj.7601378

Pelegrin, P., C. Barroso-Gutierrez, and A. Surprenant. 2008. P2X7 receptor differentially couples to distinct release pathways for IL-1beta in mouse macrophage. *J. Immunol.* 180:7147–7157.

Perez, A., A.C. Issler, C.U. Cotton, T.J. Kelley, A.S. Verkman, and P.B. Davis. 2007. CFTR inhibition mimics the cystic fibrosis inflammatory profile. *Am. J. Physiol. Lung Cell. Mol. Physiol.* 292:L383–L395. doi:10.1152/ajplung.00403.2005

Pillay, C.S., E. Elliott, and C. Dennison. 2002. Endolysosomal proteolysis and its regulation. *Biochem. J.* 363:417–429. doi:10.1042/0264-6021:3630417

Piwon, N., W. Günther, M. Schwake, M.R. Bösl, and T.J. Jentsch. 2000. ClC-5 Cl- -channel disruption impairs endocytosis in a mouse model for Dent's disease. *Nature.* 408:369–373. doi:10.1038/35042597

Prabhananda, B.S., and M.H. Kombrabail. 1992. Monensin-mediated transports of H+, Na+, K+ and Li+ ions across vesicular membranes: T-jump studies. *Biochim. Biophys. Acta.* 1106:171–177. doi:10.1016/0005-2736(92)90236-F

Rochdi, M., A.M. Delort, J. Guyot, M. Sancelme, S. Gibot, J.G. Gourcy, G. Dauphin, C. Gumila, H. Vial, and G. Jeminet. 1996. Ionophore properties of monensin derivatives studied on human erythrocytes by 23Na NMR and K+ and H+ potentiometry: relationship with antimicrobial and antimalarial activities. *J. Med. Chem.* 39:588–595. doi:10.1021/jm9505829

Roos, A., and W.F. Boron. 1981. Intracellular pH. *Physiol. Rev.* 61:296–434.

Schröder, B., C. Wrocklage, C. Pan, R. Jäger, B. Kösters, H. Schäfer, H.P. Elsässer, M. Mann, and A. Hasilik. 2007. Integral and associated lysosomal membrane proteins. *Traffic.* 8:1676–1686. doi:10.1111/j.1600-0854.2007.00643.x

Srinivas, S.P., A. Ong, L. Goon, L. Goon, and J.A. Bonanno. 2002. Lysosomal Ca(2+) stores in bovine corneal endothelium. *Invest. Ophthalmol. Vis. Sci.* 43:2341–2350.

Teichgräber, V., M. Ulrich, N. Endlich, J. Riethmüller, B. Wilker, C.C. De Oliveira-Munding, A.M. van Heeckeren, M.L. Barr, G. von Kürthy, K.W. Schmid, et al. 2008. Ceramide accumulation mediates inflammation, cell death and infection susceptibility in cystic fibrosis. *Nat. Med.* 14:382–391. doi:10.1038/nm1748

Thiagarajah, J.R., Y. Song, P.M. Haggie, and A.S. Verkman. 2004. A small molecule CFTR inhibitor produces cystic fibrosis-like submucosal gland fluid secretions in normal airways. *FASEB J.* 18:875–877.

Van Dyke, R.W. 1993. Acidification of rat liver lysosomes: quantitation and comparison with endosomes. *Am. J. Physiol.* 265:C901–C917.

Zall, D.M., D. Fisher, and M.Q. Garner. 1956. Photometric determination of chlorides in water. *Anal. Chem.* 28:1665–1668. doi:10.1021/ac60119a009